Inorganic Chemistry

Article

pubs.acs.org/IC

Supraicosahedral Polyhedra in Metallaboranes: Synthesis and Structural Characterization of 12-, 15-, and 16-Vertex Rhodaboranes

Dipak Kumar Roy,[†] Bijan Mondal,[†] Pritam Shankhari,[†] R. S. Anju,[†] K. Geetharani,[†] Shaikh M. Mobin,[‡] and Sundargopal Ghosh*[,†]

[†]Department of Chemistry, Indian Institute of Technology Madras, Chennai 600 036, India

[‡]Department of Chemistry, Indian Institute of Technology Indore, Indore 452 017, India

Supporting Information

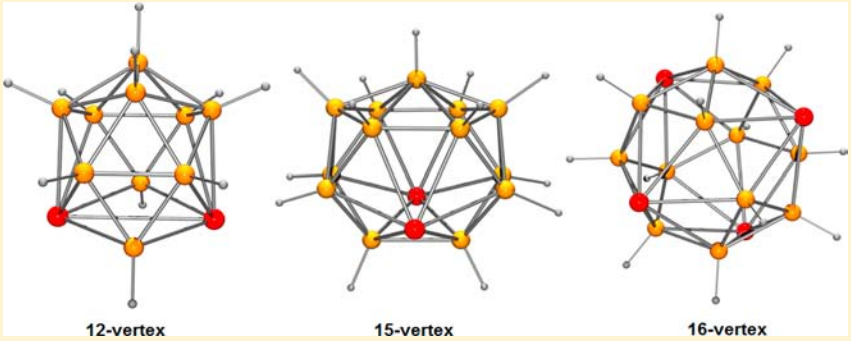

ABSTRACT: Syntheses and structural characterization of supraicosahedral rhodaborane clusters are reported. Reaction of $[(Cp^*RhCl_2)_2]$, ($Cp^* = \eta^5$-C_5Me_5) with $[LiBH_4{\cdot}thf]$ followed by thermolysis with excess of $[BH_3{\cdot}thf]$ afforded 16-vertex *closo*-$[(Cp^*Rh)_3B_{12}H_{12}Rh\{Cp^*RhB_4H_9\}]$, **1**, 15-vertex $[(Cp^*Rh)_2B_{13}H_{13}]$, **2**, 12-vertex $[(Cp^*Rh)_2B_{10}H_n(OH)_m]$, (**3a**: $n = 12$, $m = 0$; **3b**: $n = 9$, $m = 1$; **3c**: $n = 8$, $m = 2$) and 10-vertex $[(Cp^*Rh)_3B_7H_7]$, **4**, and $[(Cp^*Rh)_4B_6H_6]$, **5**. Cluster **1** is the unprecedented 16-vertex cluster, consists of a sixteen-vertex $\{Rh_4B_{12}\}$ with an *exo*-polyhedral $\{RhB_4\}$ moiety. Cluster **2** is the first example of a carbon free 15-vertex supraicosahedral metallaborane, exhibits icosihexahedron geometry (26 triangular faces) with three degree-six vertices. Clusters **3a-c** have 12-vertex *isocloso* geometry, different from that of icosahedral one. Clusters **4** and **5** are attributed to the 10-vertex *isocloso* geometry based on 10-vertex bicapped square antiprism structure. In addition, quantum-chemical calculations with DFT methods at the BP86 level of theory have been used to provide further insight into the electronic structure and stability of the optimized structures which are in satisfactory agreement with the structure determinations. All the compounds have been characterized by IR, ^1H, ^{11}B, ^{13}C NMR spectroscopy in solution, and the solid state structures were established by crystallographic analysis of compounds **1**−**5**.

INTRODUCTION

The remarkably high stability, bonding, and aromaticity of the *closo*-borane dianions, $B_nH_n^{2-}$ (n = 5−12), have been recognized for long time.[1,2] Lipscomb, Schleyer, and others reported that the *closo*-borane dianions generally become more favorable with increasing cluster size, for example, $B_{14}H_{14}^{2-}$ and $B_{17}H_{17}^{2-}$ were predicted to be more stable than $B_{11}H_{11}^{2-}$, $B_9H_9^{2-}$, and even $B_{10}H_{10}^{2-}$.[2−4] Although a number of 13-vertex metallacarboranes have been reported,[5−7] the parent supra-icosahedral homoatomic boranes (i.e., $B_nH_n^{2-}$, $n \geq 13$) are still unidentified.[8] Isoelectronic supraicosahedral carboranes of the type $C_2B_{n-2}H_n$ ($n > 12$) are more tractable synthetic objectives from a practical point of view. However, the first success was achieved in 2003 with the discovery of 13-vertex carborane by Welch.[7a] As a result, a considerable challenge in recent years is the progress of supraicosahedral borane clusters.[6,7,9] The discovery of 13-vertex heteroborane clusters,[7a] subsequently opened the door for the successful synthesis of 14 and 15-vertex metallacarboranes in 2005 and 2006 respectively,[6c,7b] and very recently 16-vertex metallaborane.[10] Although computational studies recommended stability for boron cages with 15 vertices or more, all attempts till date to prepare these clusters have very little success.

Among the hundreds of metallaboranes and their derivatives reported by Fehlner,[11] Kennedy[12] and others,[13−15] there are only a few mono- or dimetallaboranes with 12-vertices[16] known and none with more vertices. Several approaches for the synthesis of larger clusters containing main group or transition metal fragments have received substantial attention.[16−19] The most optimum and convenient synthetic method for the construction of higher nuclearity metallaborane clusters is the condensation of metal polychlorides using $[LiBH_4{\cdot}thf]$, followed by the thermal expansion with $[BH_3{\cdot}thf]$.[16a,b] Disappointingly, in most of the cases, the great majority of metallaboranes are generated in low yield with low metal to

Received: March 27, 2013
Published: May 20, 2013

   dx.doi.org/10.1021/ic400761z | *Inorg. Chem.* 2013, 52, 6705−6712

Scheme 1. Synthesis of Rhodaboranes 1−5

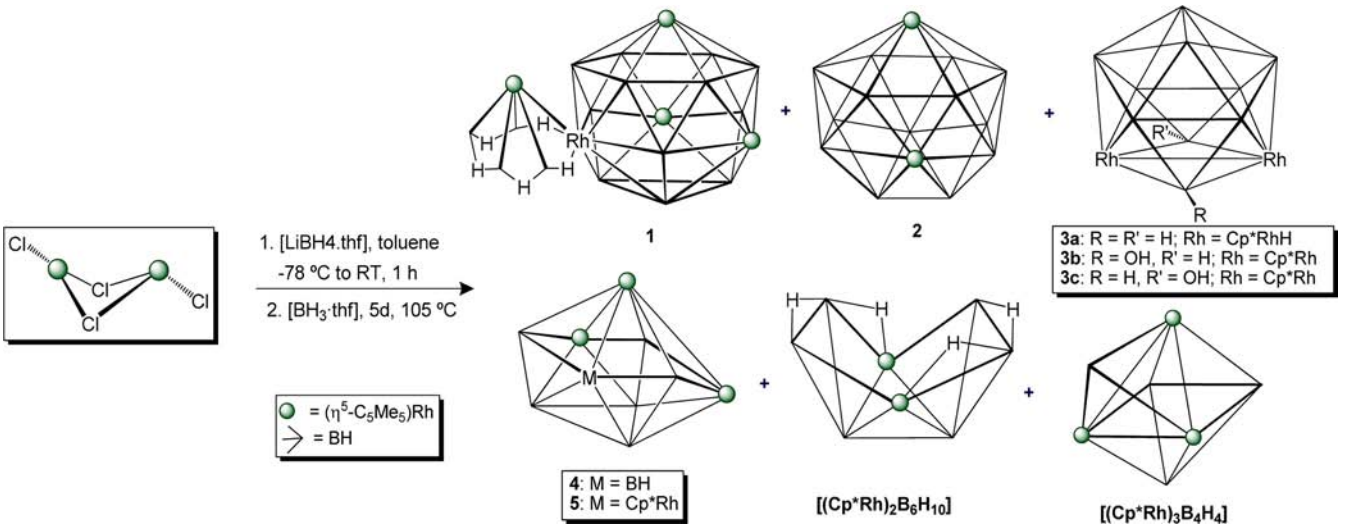

boron ratio.[16a,20] Nevertheless, applying this methodology, we have synthesized a number of new metallaboranes and their derivatives.[21,22]

In terms of systematic cluster expansion in metallaborane, the most versatile metals are rhenium[16a] and ruthenium,[16b] where known M_2B_n (M = Re, Ru) frameworks run from n = 4 to 10. Aggressive reaction of $[(Cp^*M)_2B_4H_8]$, (Cp^* = η^5-C_5Me_5; M = Re, Ru) with monoborane reagents led to the isolation of hypoelectronic *closo*-rhenaboranes $[(Cp^*Re)_2B_nH_n]$, n = 7−10,[16a] and hydrogen-rich ruthenaboranes, $[(Cp^*Ru)_2B_nH_{12}]$, n = 6, 8,[16b] and $[(Cp^*Ru)_2B_{10}H_{16}]$.[16c] The lack of larger metallaboranes has led us to renewed experimental efforts to achieve higher nuclearity clusters. As a result, we extended the approach of rhenium and ruthenium system to rhodium, and we have recently shown that it is likely to break the critical 15 to 16-vertex barrier in polyhedral boron chemistry.[10] A reinvestigation of the Rh-system, thus, resulted in a 15-vertex $[(Cp^*Rh)_2B_{13}H_{13}]$, **2**, and 12-vertex rhodaboranes, $[(Cp^*Rh)_2B_{10}H_n(OH)_m]$ (**3a**: n = 12, m= 0; **3b**: n = 9, m = 1; **3c**: n = 8, m = 2), along with a 16-vertex, *isocloso*-$[(Cp^*Rh)_3B_{12}H_{12}Rh\{Cp^*RhB_4H_9\}]$, **1**.[10] With a geometry based on a supraicosahedral framework, clusters **1** and **2** provide carbon-free example that demonstrates an additional structure type.

RESULTS AND DISCUSSION

Synthesis and Structural Characterization of Rhodaboranes 1−5. The formation of novel rhodaborane compounds **1**−**5** (Scheme 1) proceeds via the reaction between $[Cp^*RhCl_2]_2$ and excess of $[LiBH_4{\cdot}thf]$ followed by thermolysis with excess of $[BH_3{\cdot}thf]$ at 105 °C for five days. In parallel to the formation of **1**−**5**, known rhodaboranes ($[(Cp^*Rh)_2B_6H_{10}]$,[20a] $[(Cp^*Rh)_2B_8H_{12},]$[20a] and $[(Cp^*Rh)_3B_4H_4]$[20c]) have also been isolated in moderate yields. Following is the detail spectroscopic and structural characterization of the novel rhodaboranes.

16- and 15-Vertex Rhodaboranes 1 and 2 (1: $[(Cp^*Rh)_3B_{12}H_{12}Rh\{Cp^*RhB_4H_9\}]$ and 2: $[(Cp^*Rh)_2B_{13}H_{13}]$). A preliminary account of the synthesis and structural analysis of 16-vertex rhodaborane *closo*-$[(Cp^*Rh)_3B_{12}H_{12}Rh\{Cp^*RhB_4H_9\}]$, **1**, has been communicated earlier.[10] Compound **1** represents the first example of 16-vertex M_4B_{12} boron cluster, the solid state structure (Figure 1) showed that its Rh_4B_{12} architecture of crystallographic C_s

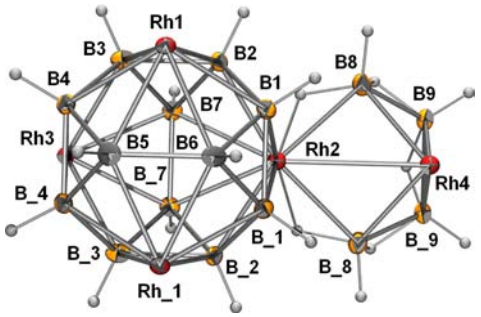

Figure 1. Crystallographically derived X-ray structure representations of *closo*-$[(Cp^*Rh)_3B_{12}H_{12}Rh\{Cp^*RhB_4H_9\}]$, **1**. Cp* ligands are excluded for clarity. Selected bond lengths (Å) and angles (deg): Rh2−B1 2.234(4), Rh2−B7 2.258(4), Rh2−B8 2.350(5), Rh2−Rh4 2.8751(6), B5−B4 1.779(6), Rh3−B7 2.214(4), Rh3−B4 2.0.220(4); B6−B1−B1 59.84(16), B6−B1−B2 119.5(3), B1−B1−B2 119.79(18), B6−B1−Rh1 65.99(19), B6−B1−Rh2 119.1(2), B1−B1−Rh2 66.40(10), B2−B1−Rh2 66.53(18), Rh1−B1−Rh2 124.62(19).

symmetry consists of a centered icosioctahedron (or 28-hedron) core and the exopolyhedral $\{Cp^*RhB_4H_9\}$ fragments that attached to one of the rhodium atoms of Rh_3B_3 belt in η^5 fashion. Compound **1** possesses a C_s symmetry consistent with the $^{11}B\{^1H\}$ NMR resonances between δ 37 and 5 ppm (6:6:2:2) in solution. Presumably, because of the coordination environment, the 12 cage boron atoms displayed resonances in 6:6 intensity ratio in $^{11}B\{^1H\}$ NMR spectrum. In addition to a single resonance for three cage Cp* protons and the exopolyhedral Cp* protons, the ^1H NMR spectrum of **1** shows two broad resonances at δ −2.35, −3.13 ppm for the B−H−B bridging protons of the exopolyhedral fragment and one resonance at δ − 6.54 ppm for two Rh−H−B bridging hydrides. The variable temperature $^1H\{^{11}B\}$ and $^{11}B\{^1H\}$ NMR evidence no fluxional behavior of **1**, in particularly the *exo*-polyhedral unit.

The molecular structure of **2**, shown in Figure 2, comprises a 15-vertex polyhedron with a degree-six Rh atom bound to the upper hexagonal B_6 belt (B1−B6), below which is an antiprismatic RhB_5 belt (Rh2−B11). Lower than this, in turn,

dx.doi.org/10.1021/ic400761z | Inorg. Chem. 2013, 52, 6705−6712

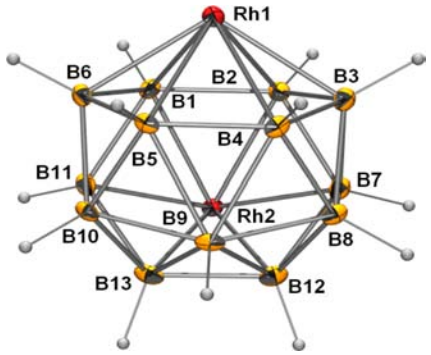

Figure 2. Molecular structure of $[(Cp^*Rh)_2B_{13}H_{13}]$, **2** (the Cp* ligands are excluded for clarity). Selected bond lengths (Å): B1−Rh1 2.212(4), B4−Rh1 2.232(6), B1−B6 1.774(6), B5−B6 1.751(8), B5−B9 1.934(9), B7−B8 1.813(8), B7−Rh2 2.190(5), B11−Rh2 2.179(5); B6−B1−Rh2 116.8(3), B11−B1−Rh2 65.0(2), Rh1−B1−Rh2 120.16(18), B8−B4−B3 62.8(4), B13−B12−Rh2 66.6(2), B3−Rh1−B2 47.15(18).

sits the B12 and B13 atoms. The polyhedral structure of **2** is related to the D_{3h} symmetry with a C_3 axis passing through the centers of the B3−B7−B8 and B6−B10−B11 planes, if the differences among the Rh and B atoms are ignored. This geometry is similar to that predicted for the parent borane $[B_{15}H_{15}]^{2-}$.[3a] Cluster **2** contains three degree-six vertices (Rh1, Rh2, and B9). However, the 15-vertex ruthenacarborane reported by Welch contains only two degree-six vertices with a missing connectivity (B−C). Thus, it generates a quadrilateral face, and the polyhedron geometry is pentacosahedron (25 faces).[7b] On the other hand, cluster **2** adopts a *closo* structure with 26 triangular faces, and thus it can be considered as hexacosahedron or icosihexahedron (26-hedron). The most interesting features of this structure are the coplanar B_6 bonding face and the chair conformation of the RhB_5 bonding face (Rh2−B7−B8−B9−B10−B11) (Figure 2). In this sandwich-type molecule, the Cp* ring is parallel to the hexagonal bonding face (B1−B6) with an Rh-Cp*(cent) distance of 1.89 Å and Rh−B_6(cent) distance of 1.31 Å, which are comparable to the corresponding values of 1.78 and 1.41 Å in 15-vertex metallacarborane 1,4-$(CH_2)_3$-7-(*p*-cymene)-7,1,4-$RuC_2B_{12}H_{12}$.[6c] The average Rh−cage boron atom distance of 2.206 Å is comparable to the corresponding value of 2.247(3) Å in 15-vertex metallacarborane.[6c] The B−B bond distances within **2** follow the trends established for supraicosahedral clusters.[6,7]

The mass spectrum of cluster **2** shows a molecular ion peak (ESI^+) at 629, corresponding to $C_{20}H_{43}B_{13}Rh_2$, while the IR spectrum displays a band at 2464 cm^{-1} due to the terminal B−H stretches. Both the ^1H and ^{11}B NMR spectra of **2** at 298 K are consistent with time-averaged molecular C_s symmetry. The ^{11}B NMR spectrum displays five resonances with an intensity ratio of 4:2:2:4:1, distributed over an unusually large chemical shift range. Further, the computed ^{11}B chemical shift values of **2** using gauge-including atomic orbital density functional theory [GIAO−DFT] method at the B3LYP/def2-TZVP level follow a suitable trend with the experimental values (Supporting Information, Table S1). In addition, the ^1H and ^{13}C NMR spectra exhibit a consistent symmetry pattern.

Polyhedral expansion, a method invented by Hawthorne,[17a] has been widely used in the preparation of supraicosahedral metallacarboranes.[6,7,17,23] Although the 15-vertex metallacarboranes have been known for some time,[6c,7b] an analogous metallaborane cluster was not known till now. To the best of our knowledge, cluster **2** is the first example of a neutral 15-vertex carbon free cluster, analogous to 15-vertex metallacarborane. This 15-vertex cluster can be viewed as a truncated tricapped trigonal prism.[24,25] Alternatively, capping of the open pentagonal face of 14-vertex cluster $[(\eta^5\text{-}C_5H_5)_2Fe_2(CH_3)_4C_4B_8H_8]$ of Grimes also forms structure **2**.[17b] Further, *closo*-15-vertex cluster without any substituents are found in BeB_3[25] and SiB_6.[26] Precedent for this structure is also found in metal alloy crystal structures.[27]

Following the skeletal electron-counting rules,[15] the cluster **2** with a 15-vertex deltahedral geometry requires 16 skeletal electron pairs (sep), while 15 sep are available for **2**. It may, thus, be considered as a 2*n* skeletal electron *isocloso* system.[28] Here, we should mention that the hexacosahedron cluster **2** qualifies as a *closo*-polyhedron according to the criteria for it.[29] The supraicosahedral boranes and carboranes with deltahedral structures essentially have one or more vertices of degree-six. In such structures it has been noted that, {BH} vertices are not mostly well-suited to degree-six as their valence orbitals are not diffused.[7] Out of three degree-six vertices in **2**, one of the vertices is occupied by boron that stabilizes the supraicosahedral geometry and eliminates the need for structural distortion.[7b]

The DFT calculations have been carried out to study the electronic structure of **2′** (Cp analogue of **2**, Supporting Information, Figure S1). The results are compared and contrasted with the highest occupied molecular orbital (HOMO) of non-Wadian $[B_{15}H_{15}]$ and Wadian $[B_{15}H_{15}]^{2-}$ molecules (Figure 3 and Supporting Information, Figures S2 and S3). As shown in Figure 3, the HOMO is bounded strongly

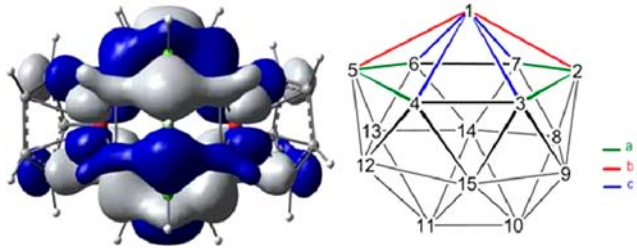

Figure 3. HOMO of **2′** (Cp analogue of **2**).

along 2−3, 2−7, 5−4, and 5−6 edges (*a*); fairly strong along 1−5 and 1−2 edges (*b*). However, it bonded weakly with 1−4, 1−6, 1−3, and 1−7 edges (*c*). The average bond lengths of a, b, and c are 1.739 Å, 1.790 Å, and 1.922 Å, respectively. Interestingly, a similar situation has also been observed in $[B_{15}H_{15}]$, where the average B−B bond lengths are 1.755 Å, 1.854 Å, and 1.923 Å, respectively. The pertinent DFT-optimized bond distances of the model clusters are listed in Supporting Information, Table S2. The DFT studies further show greater thermodynamic stability of **2′** over the *isocloso*-$[B_{15}H_{15}]$.[30] Indeed, a large HOMO−LUMO gap of **2′** as compared to **2″** [(*closo* **2**)$^{2-}$] supports the *isocloso* description of **2** (ca. 2.34 and 1.27 eV for **2′** and **2″**) (Table 1).

12-Vertex Rhodaboranes $[(Cp^*Rh)_2B_{10}H_n(OH)_m]$, 3a-c: (3a: *n* = 12, *m* = 0; 3b: *n* = 9, *m* = 1; 3c: *n* = 8, *m* = 2). Compounds **3a−c** were isolated, as air-stable yellow solids. The solid-state X-ray structure of **3a**, shown in Figure 4, adopts a 12 vertex geometry different from that of the icosahedral core. The observed shape can be related to the canonical deltahedra by one DSD (diamond square diamond) rearrangement keeping

dx.doi.org/10.1021/ic400761z | *Inorg. Chem.* 2013, 52, 6705−6712

Table 1. Calculated HOMO and LUMO Energies (eV), HOMO-LUMO Gaps ($\Delta E = E_{LUMO} - E_{HOMO}$, eV) and NICS(0) (ppm) for $[B_{15}H_{15}]$, 2a, 2′, and 2″ at the BP86/def2-TZVP Level

	$[B_{15}H_{15}]$	2a	2′	2″
HOMO	−7.91	−5.80	−5.96	2.84
LUMO	−6.08	−3.06	−3.62	4.11
ΔE	1.83	2.74	2.34	1.27
NICS(0)	−12	−14.9	−11.1	

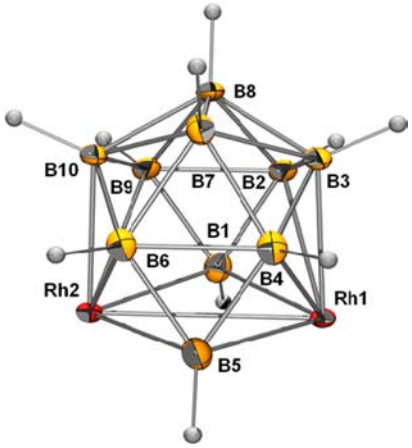

Figure 4. Molecular structure of $[(Cp^*Rh)_2B_{10}H_{12}]$, **3a** (the Cp* ligands are excluded for clarity). Selected bond lengths (Å): Rh1−Rh2 2.9546(7), B1−B2 1.683(14), B1−Rh1 2.137(9), B3−B4 1.760(14), B2−B9 1.779(12), B2−Rh1 2.260(7); B2−B1−B9 63.0(6), B2−B1−Rh1 71.4(5), B9−B1−Rh2 69.1(4), B1−B2−B9 59.3(5), B1−B2−Rh1 63.7(4), B7−B3−B2 110.8(7), B7−B3−B4 59.8(6).

the total vertex connectivities (tvc) same (Supporting Information, Figure S6). Although, the connectivity pattern of **3a** is consistent with *hypercloso* geometry, it has (n + 1) sep obeying the Wade−Williams relationship.[15] The average Rh−B and B−B bond lengths are consistent with other dirhodaboranes;[20] however, the Rh−Rh bond length in **3a** (2.9546(7) Å) is significantly longer (ca. 0.26 Å). This lengthening of bond length may be due to the presence of two hydride ligands bound to the metal center (Wiberg bond indices (WBI) of 0.41 that corresponds to coupling of Rh1 with Rh2, Supporting Information, Figure S7, S8). The location of hydride ligands has been confirmed by ^{1}H NMR spectroscopy.

The $^{11}B\{^1H\}$ NMR chemical shift pattern (2:2:4:2) of **3a** suggests a structure of higher symmetry, which is further supported by the $^1H\{^{11}B\}$ NMR spectrum that exhibits one type of Cp* protons at δ 1.82 ppm. In addition to the resonances due to BH terminal protons, the ^{1}H NMR spectrum reveals sharp resonances in the hydride region which shows coupling to ^{103}Rh [J(RhH) < 1 Hz] centered at δ −24.37 ppm. Thus, the resonance is typically arising from a Rh−H hydride. In a further attempt to confirm these assignments, a 2D $^1H\{^{11}B\}/^{11}B\{^1H\}$ HSQC experiment was performed, which is consistent with the structure of **3a**. As far as we are aware, cluster **3a**, next to $[(Cp^*Re)_2B_{10}H_{10}]$,[31] represents the second example of a 12-vertex metallaborane with a cross cluster M-M bond.

Compounds **3b** and **3c** are attributed to the 12-vertex *isocloso* geometry. The core geometry and the basic structural features of **3b** and **3c** are very similar, the essential difference is the position of the OH group(s) (Figure 5). Crystallographic

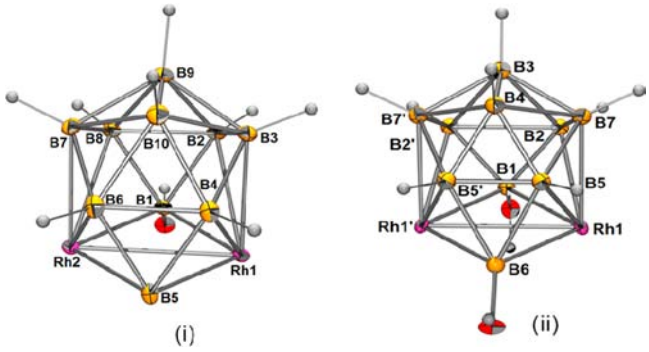

Figure 5. Molecular structure and labeling diagram of (i) $[(Cp^*Rh)_2B_{10}H_9(OH)]$, **3b** and (ii) $[(Cp^*Rh)_2B_{10}H_8(OH)_2]$, **3c**. Cp* ligands are excluded for clarity. Selected bond lengths [Å] and angles [deg] for **3b**: Rh1−Rh2 2.8040(6), B1−B8 1.781(9), B1−Rh1 2.157(6), B1−O1A 1.372(7); O1A−B1-B8 126.4(5), B8 B1 B2 59.5(3), B8−B1−Rh2 68.4(3), B3 B4 Rh1 67.1(3). **3c**: Rh1−Rh1′ 2.811(2), B6−Rh1 2.22(3), B5−B7 1.55(4), B5−B5 1.99(7), B2−B2 1.57(6), B6−O2 1.327(18); O1−B1−B2 120(3), B2−B1−B2 50(2), O1−B1−Rh1 130.1(19), B2−B1−Rh1 71.8(13), B1−B2−B7 115(2).

structure of **3b** was solved using the program SIR-92 and refined using SHELX-97.[32] Boron B1 and B5 showed different peaks satisfying the B−O distance. These peaks were assigned as oxygen, and their occupancies were released as parameters for refinement. The refinement of the occupancies showed that the sum of their occupancies is nearly one. The final refinement cycle showed the relative occupancies of OH oxygen as O1A (0.763) and O1B (0.237). Hence, it is inferred that the molecule **3b** contains one OH-group disordered at two positions of the crystal, whereas, in **3c** two OH groups are attached to B1 and B6 atoms.

Although the average B−B (1.79 Å) and Rh−B bond lengths (2.05 Å) in **3c** are comparable to those observed in rhodaborane clusters,[20] the anomalous B−B and Rh−B indicates the displacement of *closo* to *isocloso* structure. The observed geometry of **3b** and **3c** can be related to the canonical ones by one dsd rearrangement, consequently making the total vertex connectivity (tvc) same to the canonical deltahedra. The 12-vertex clusters **3b** and **3c** are two electrons short of the expected electron count for a *closo* cluster and therefore are consistent with a *hypercloso* rather than *closo* metallaborane species. The change in the structural parameters of cluster **3a-c** may be due to the presence of OH group(s) in the cluster(s).

The $^{11}B\{^1H\}$ NMR spectrum of **3b** shows seven types of ^{11}B NMR signals ranging from δ 87 to −19 ppm whereas, **3c** exhibits near-coalescence, with four broad resonances at δ 87, 26, 4.7, −13.3 ppm. The IR spectrum of **3b** and **3c** feature bands at 1376 and 1344 cm^{-1} in a region characteristic of the B−O and band at 3610, 3613 cm^{-1} corresponds to O−H stretching frequency, respectively. Although, we are unable to provide any direct reason for the presence of oxygen in **3b** and **3c**, it has previously been observed in other polyborane/$[\{Cp^*RhCl_2\}_2]$[33−35] systems when handled in air. Therefore, the trace amount of water/air bound to the silica gel leads to the incorporation of oxygen atoms in **3b** and **3c**.

Metallaboranes **3a-c** are the new examples of polyhedral boron containing compounds; those are similarly anomalous to other 12 vertex metallaboranes, and may therefore shed additional light on their structures. A set of three metallaboranes (types **I-III**) containing M_2B_{10} framework of group 6−10 metals are shown in Chart 1. They are $[(PMe_2Ph)_4)$-

dx.doi.org/10.1021/ic400761z | Inorg. Chem. 2013, 52, 6705−6712

Chart 1. Twelve Vertex Metallaboranes[a]

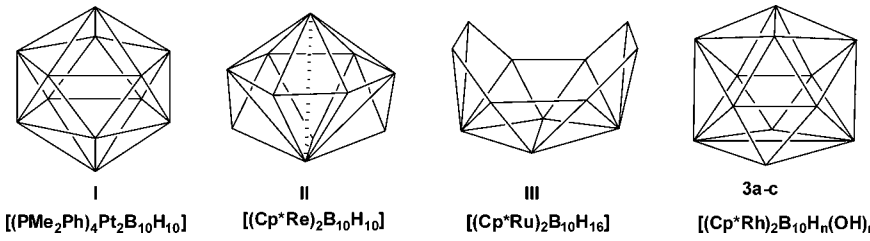

[a]Bridging hydrogen atoms are not shown for clarity.

$Pt_2B_{10}H_{10}$],[16d] **I**, [$(Cp^*Re)_2B_{10}H_{10}$],[31] **II**, and [$(Cp^*Ru)_2B_{10}H_{16}$],[16b] **III**. The observed geometry of **I** is same as that of the canonical deltahedra of $[B_{12}H_{12}]^{2-}$. The isostructural metallaborane type **II** can be related to the canonical ones by diamond-square-diamond (dsd) rearrangements. The diruthenaborane cluster type **III** on the other hand can be derived from a capped truncated tetrahedron of a type where two metal atoms occupy two of the four hexagonal faces. The molecular structure of these compounds reveals that they have different geometries despite having the same number of borane fragments. Clusters **3a-c** may thus be considered as the next members of this series containing an M_2B_{10} framework.

10-Vertex Rhodaboranes 4 and 5 (4: [$(Cp^*Rh)_3B_7H_7$] and 5: [$(Cp^*Rh)_4B_6H_6$]). The constituents of **4** and **5** were determined by an X-ray diffraction study of a suitable single crystal grown from analytically pure compound by slow evaporation from hexane solution at −10 °C (Figure 6).

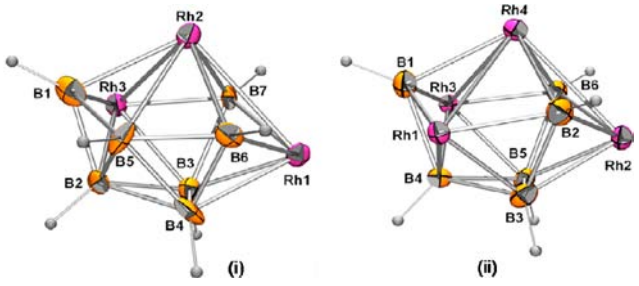

Figure 6. Molecular structure and labeling diagram of (i) **4** and (ii) **5**. Cp* ligands are excluded for clarity. Selected bond lengths [Å] and angles [deg] for **4**: Rh1−Rh2 2.8144(18), B7−Rh3 2.010(16), B6−Rh2 2.186(16), B3−B7 1.86(2); B2−B1−B5 61.8(12), B2−B1−Rh2 102.3(13), B5−B1−Rh2 69.9(10). Selected bond lengths [Å] and angles [deg] for **5**. Rh2−Rh4 2.7944(4), Rh1−Rh4 2.8013(4), B6−Rh3 2.069(4), B2−B3 1.903(6), B5−B4−B1 111.9(3), B1−B4−Rh1 60.38(16), B4−B3−Rh1 66.27(19).

Compound **4** crystallizes in the triclinic space group $P\bar{1}$, and the coordination sphere of the metal centers are satisfied by the Cp* ligands. Figure 6 represents a novel 10-vertex closed geometry and shows that the Rh_2B_7 cage by its 6-membered (Rh_2B_4) open face coordinated to the unique Rh atom of cluster connectivity six. Compound **4** is attributed to the 10-vertex *isocloso* geometry similar to that of our recently reported compound **5**.[10] Both the structures are based on a 10-vertex *closo* bicapped square antiprism (electron precise closo type) by one diamond square diamond (DSD) rearrangement. The average Rh−Rh separation in **4** (2.814 Å) is longer than that found in **5** (2.792 Å) while the average B−B (1.74 Å) and Rh−B bond lengths (2.14 Å) follow the rhodaboranes trend.[20] But the disparity in bond length between boron atoms (ranging from 1.69 to 1.86 Å) may be due to the *isocloso* nature of the framework. The six-membered face of **4** is slightly distorted from a regular chair conformation as the absolute values of torsion angles about the bonds of the 6-membered cycle vary from 40.4 to 52.4°; whereas, for **5** it is 51.8−52.8°. The change in the structural parameters between **4** and **5** might be due to the presence of an extra metal center in the six-membered ring of compound **5**.

The $^{11}B\{^1H\}$ NMR spectrum displayed four resonances which is in full agreement with the X-ray analysis. This may be due to the overlapping of the similar boron environments. The ^1H NMR spectrum of **1** features two Cp* resonances at δ 1.83 and 1.68 ppm in the ratio of 1:2. The IR spectrum shows absorption at 2429 and 2491 cm^{-1} for terminal B−H stretches.

The core skeleton of clusters **4** and **5** are same as the other 10-vertex *isocloso* structures having 10 sep with different numbers of metal atoms (Chart 2). A remarkable series of superelectron-deficient 10-vertex *hypercloso*-metallacarborane clusters[36] as well as closely related *isocloso*-metallaboranes[37] have been systematically prepared and investigated both experimentally and theoretically by Hawthorne, Kennedy, and King and co-workers. However the metal rich *isocloso*-rhodaboranes **4** and **5** having three and four metal fragments, respectively, in the cluster were previously unknown for the 10-vertex *isocloso* geometry.

Although it is difficult to study the pathway for the formation of these higher-vertex clusters, the core geometries of compounds **1**−**5** provide some insights on the generation of these novel compounds. Note that clusters **1**−**5** contain either Rh_2B_6 or Rh_2B_8 core, similar to that observed in

Chart 2. Metallaboranes with *isocloso* Geometry

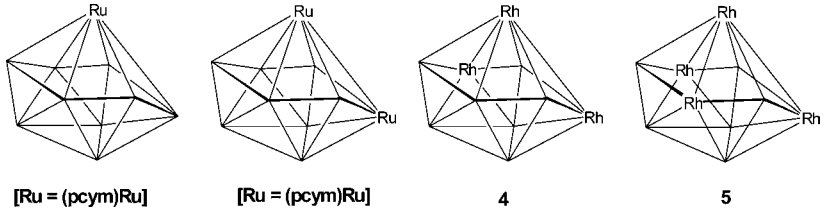

dx.doi.org/10.1021/ic400761z | Inorg. Chem. 2013, 52, 6705−6712

$[(Cp^*Rh)_2B_6H_{10}]$ or $[(Cp^*Rh)_2B_8H_{12}]$ respectively. Therefore, the formation of these clusters may be considered as cluster growth reaction by borane or metal fragment(s) addition external to the cluster framework of $[(Cp^*Rh)_2B_6H_{10}]$ or $[(Cp^*Rh)_2B_8H_{12}]$. However, all of our attempts to insert BH fragments into $[(Cp^*Rh)_2B_6H_{10}]$ or $[(Cp^*Rh)_2B_8H_{12}]$ failed to produce higher vertex clusters **1**−**5**.

CONCLUSION

The results described herein demonstrate the first structural characterization of supraicosahedral neutral metallaborane clusters. Among the several methods for the formation of supraicosahedral clusters recognized, the overall applicability of this route would be vital since, to the best of our knowledge, this offers for the first time the synthesis of supraicosahedral metallaborane clusters by M−X, B−H bond metathesis. Finally, the synthesis and ongoing investigation of the chemistry of rhodaboranes, in particular synthesis of higher nuclearity rhodaborane, represents a stirring development in metallaborane chemistry. Such approaches may allow the generation of supraicosahedral metallaboranes of other group 9 metals.

EXPERIMENTAL SECTION

General Procedures and Instrumentation. All syntheses were carried out under an argon atmosphere with standard Schlenk and glovebox techniques. Solvents were dried by common methods and distilled under N_2 before use. $[Cp^*RhCl_2]_2$, $[BH_3{\cdot}thf]$, and $[LiBH_4{\cdot}thf]$ (Aldrich) were used as received. The external reference for the ^{11}B NMR, $[Bu_4N(B_3H_8)]$, was synthesized with the literature method.[38] Thin layer chromatography was carried on 250 mm dia aluminum supported silica gel TLC plates (MERCK TLC Plates). NMR spectra were recorded on a 400 and 500 MHz Bruker FT-NMR spectrometer. Residual solvent protons were used as reference (δ, ppm, $[D_6]$-benzene, 7.16), while a sealed tube containing $[Bu_4N(B_3H_8)]$ in $[D_6]$benzene (δ_B, ppm, −30.07) was used as an external reference for the ^{11}B NMR. Infrared spectra were recorded on a Nicolet iS10 spectrometer. The microanalyses for C and H were performed on Perkin Elmer Instruments series II model 2400. The mass spectra were recorded on Bruker MicroTOF-II mass spectrometer.

Synthesis of 1−5. To a flame-dried Schlenk tube $[Cp^*RhCl_2]_2$ (0.21 g, 0.34 mmol) was suspended in toluene (15 mL) and cooled to −78 °C, $[LiBH_4{\cdot}thf]$ (2.0 mL, 3.49 mmol) was added, and the reaction mixture was allowed to warm slowly to room temperature and left stirring for an additional hour. The intermediate was extracted in hexane, and the filtrate solution was thermolyzed at 105 °C in presence of $[BH_3{\cdot}thf]$ (3.5 mL, 3.5 mmol) for 5 days. The solvent was dried, and the residue was extracted into hexane and subjected to chromatographic work up using silica gel TLC plates. Elution with a hexane/CH_2Cl_2 (75:25 *v*/*v*) mixture yielded yellow **1** (0.064g, 15%), red **2** (0.022g, 10%), and yellow **3a** (0.012g, 6%), yellow **3b** (0.007g, 3%), yellow **3c** (0.009g, 4%), orange **4** (0.015g, 5%), and green **5** (0.029g, 8%) along with known rhodaboranes $[(Cp^*Rh)_2B_6H_{10}]$, (0.015g, 8%), $[(Cp^*Rh)_2B_8H_{12}]$, (0.003g, 12%) and $[(Cp^*Rh)_3B_4H_4]$, (0.004g, 15%). These known rhodaboranes have been characterized by comparison of their spectroscopic data reported earlier.[20]

1. MS (ESI$^+$) = 1248. ^{11}B NMR (22 °C, 128 MHz, d_6-benzene): δ 37.1 (d, 6B), 35.0 (d, 6B), 24.3 (d, 2B), 4.9 (d, 2B). ^1H NMR (22 °C, 400 MHz, d_6-benzene): δ 4.88 (partially collapsed quartet (pcq), 6 BH_t), 4.53 (pcq, 4 BH_t), 4.12 (pcq, 4 BH_t), 3.86 (pcq, 2 BH_t), 1.70 (s, 15H; 1Cp*), 1.67 (s, 45H; 3Cp*), −2.35 (br, 2H; B−H−B), −3.13 (br, 1H; B−H−B), −6.54 (br, 2H; Rh−H−B). ^{13}C NMR (22 °C, 100 MHz, d_6-benzene): δ 103.5, 101.3 ($C_5(CH_3)_5$), 9.6, 9.1 ($C_5(CH_3)_5$). IR (hexane) ν/cm^{-1}: 2475w (BH_t). Elemental analysis (%) calcd for $C_{40}H_{81}B_{16}Rh_5$: C, 38.45; H, 6.53. Found: C, 38.18; H, 6.33.

2. MS (ESI$^+$) = 629. ^{11}B NMR (22 °C, 128 MHz, d_6-benzene): δ 58.6 (d, 4B), 22.0 (d, 2B), 19.9 (d, 2B), 4.7 (d, 4B), −42.0 (d, 1B). ^1H NMR (22 °C, 400 MHz, d_6-benzene): δ 5.56 (partially collapsed quartet (pcq), 4H; BH_t), 4.81 (pcq, 2H; BH_t), 3.69 (pcq, 2H; BH_t), 3.21 (pcq, 4H; BH_t), 2.51 (pcq, 1H; BH_t), 1.61 (s, 30H; 2Cp*). ^{13}C NMR (22 °C, 100 MHz, d_6-benzene): δ 102.3 ($C_5(CH_3)_5$), 10.0 ($C_5(CH_3)_5$). IR (hexane) ν/cm^{-1}: 2464w (BH_t).

3a. MS (FAB): *m*/*z* P^+_{max}: 595. ^{11}B NMR (22 °C, 128 MHz, d_6-benzene): δ 82.1 (d, 2B), 21.7 (d, 2B), 9.0 (d, 4B), −10.1 (d, 2B). ^1H NMR (22 °C, 400 MHz, d_6-benzene): δ 5.26 (partially collapsed quartet (pcq), 2H; BH_t), 4.91 (pcq, 2H; BH_t), 4.13 (pcq, 4H; BH_t), 3.32 (pcq, 2H; BH_t), 1.82 (s, 30H; 2Cp*), −24.37 (t, 2H; 2Rh−H). ^{13}C NMR (22 °C, 100 MHz, d_6-benzene): δ 100.5 ($C_5(CH_3)_5$), 11.2 ($C_5(CH_3)_5$). IR (hexane) ν/cm^{-1}: 2523w (BH_t).

3b. MS (FAB): *m*/*z* P^+_{max}: 609. ^{11}B NMR (22 °C, 128 MHz, d_6-benzene): δ 87.7 (d, 1B), 29.4 (d, 2B), 12.2 (d, 2B), 2.4 (d, 2B), −8.4 (d, 1B), −12.1 (d, 1B), −19.9 (d, 1B). ^1H NMR (22 °C, 400 MHz, d_6-benzene): δ 5.56 (partially collapsed quartet (pcq), 1H; BH_t), 5.31 (pcq, 2H; BH_t), 4.62 (pcq, 2H; BH_t), 4.22 (pcq, 1H, BHt), 4.03 (pcq, 1H, BHt), 3.91 (pcq, 2H; BH_t), 2.32 (b, 1H, OH), 1.88 (s, 30H; 2Cp*). ^{13}C NMR (22 °C, 100 MHz, d_6-benzene): δ 96.6 ($C_5(CH_3)_5$), 9.4 ($C_5(CH_3)_5$). IR (hexane) ν/cm^{-1}: 1376w (B−O), 2496w (BH_t), 3610s (O−H).

3c. MS (FAB): *m*/*z* P^+_{max}: 626. ^{11}B NMR (22 °C, 128 MHz, d_6-benzene): δ 87.4 (d, 2B), 26.9 (d, 2B), 4.7 (d, 4B), −13.3 (d, 2B). ^1H NMR (22 °C, 400 MHz, d_6-benzene): δ 4.88 (partially collapsed quartet (pcq), 2H; BH_t), 4.53 (pcq, 4H; BH_t), 4.12 (pcq, 2H; BH_t), 2.11 (b, 2H, OH), 1.70 (s, 30H; 2Cp*). ^{13}C NMR (22 °C, 100 MHz, d_6-benzene): δ 98.5 ($C_5(CH_3)_5$), 9.8 ($C_5(CH_3)_5$). IR (hexane) ν/cm^{-1}: 1344w (B−O), 2482w (BH_t), 3613w (O−H).

4. MS (FAB): *m*/*z* P^+_{max}: 795. ^{11}B NMR (22 °C, 128 MHz, d_6-benzene): δ 35.4 (d, 2B), 18.8 (d, 1B), 11.2 (d, 2B), −2.5 (d, 1B), −18.9 (d, 1B). ^1H NMR (22 °C, 400 MHz, d_6-benzene): δ 5.26 (partially collapsed quartet (pcq), 2H; BH_t), 4.91 (pcq, 2H; BH_t), 4.13 (pcq, 1H; BH_t), 3.32 (pcq, 2H; BH_t), 1.83 (s, 30H; 2Cp*), 1.68 (s, 15H; 1Cp*). ^{13}C NMR (22 °C, 100 MHz, d_6-benzene): δ 98.8, 98.1 ($C_5(CH_3)_5$), 11.6, 9.9 ($C_5(CH_3)_5$). IR (hexane) ν/cm^{-1}: 2477w (BH_t).

5. MS (ESI$^+$) = 1022. ^{11}B NMR (22 °C, 160 MHz, d_6-benzene): δ 38.7 (d, 136 Hz, 4B), 21.4 (d, 144 Hz, 2B). ^1H NMR (22 °C, 500 MHz, d_6-benzene): δ 3.26 (pcq, 2 BH_t), 2.65 (pcq, 4 BH_t), 1.78 (s, 30H; 2Cp*) 1.63 (s, 30H; 2Cp*). ^{13}C NMR (22 °C, 125 MHz, d_6-benzene): δ 103.8 ($C_5(CH_3)_5$), 9.63 ($C_5(CH_3)_5$). IR (hexane) ν/cm^{-1}: 2538w (BH_t). Elemental analysis (%) calcd for $C_{40}H_{66}B_6Rh_4$: C, 46.94; H, 6.49. Found: C, 46.56; H, 6.19.

X-ray Structure Determination. Suitable X-ray quality crystals of **1**−**5** were grown by slow diffusion of a hexane:CH_2Cl_2 solution. The crystal data for **1**, **3a**−**c**, **4**, and **5** were collected and integrated using a Bruker AXS kappa apex2 CCD diffractometer, with graphite monochromated Mo−Kα (λ = 0.71073 Å) radiation at 173 K. Crystal data for **2** was collected and integrated using Oxford Diffraction Xalibur-S CCD system equipped with graphite monochromated Mo−Kα radiation (λ = 0.71073 Å) radiation at 150 K. The structures were solved by heavy atom methods using SHELXS-97 or SIR92[32,39] and refined using SHELXL-97.[40]

DFT Calculations. Quantum chemical calculations were performed on the model compounds **2**′ and **3a**′ (Cp analogue of **2** and **3a** respectively) using density functional theory (DFT)[41] as implemented in Gaussian09[42] program package. To save computing time all the calculations were carried out with the Cp analogue model compounds, instead of Cp*. All the model compounds were fully optimized in gaseous state (no solvent effect) without any symmetry constraints using the BP86[43] functional in conjunction with the all electron triple-ζ valence def2-TZVP[44] basis set. The 28 core electrons of rhodium were replaced by the quasi-relativistic effective core potential def2-ECP[45] for rhodium. The nature of the optimized stationary point was confirmed by analytic computation of harmonic force constant. Nucleus-Independent Chemical Shifts (NICS)[46,47] and NMR chemical shifts were calculated with the hybrid Becke−Lee−Yang−Parr (B3LYP) functional,[48] using the BP86/def2-TZVP optimized geometries. Computation of the NMR shielding tensors employed gauge-including atomic orbitals (GIAOs),[49−51] using the implementation of

dx.doi.org/10.1021/ic400761z | Inorg. Chem. 2013, 52, 6705−6712

Schreckenbach, Wolff, Ziegler, and co-workers.[52−56] As a normal routine, we placed ghost atoms at the cage critical points (CCP)[57] to calculate the magnetic shielding tensor and measure aromaticity from the magnetic point of view. These values are denoted as NICS(0) as suggested by Schleyer et al.[46] Increasing aromaticity is indicated by more negative NICS values. NBO analysis was carried out using the NBO routine within the Gaussian09 package. The projected ^{11}B chemical shielding values, determined from B3LYP/def2-TZVP level of calculations, were referenced to B_2H_6 as the primary reference point, and these chemical shift values (δ) were then converted to the standard $BF_3{\cdot}OEt_2$ scale using the experimental value of +16.6 ppm for B_2H_6.

■ ASSOCIATED CONTENT

Ⓢ Supporting Information

The supplementary crystallographic data and X-ray crystallographic files for **1**−**5**. This material is available free of charge via the Internet at http://pubs.acs.org.

■ AUTHOR INFORMATION

Corresponding Author

*E-mail: sghosh@iitm.ac.in.

Notes

The authors declare no competing financial interest.

■ ACKNOWLEDGMENTS

This work was supported by the Department of Science and Technology, DST (Project No. SR/SI/IC-13/2011), New Delhi, India. Computational facilities from the IIT Madras computer center are gratefully acknowledged. D.K.R. and K.G. thank the Council of Scientific and Industrial Research (CSIR), and A.R.S. is grateful to University Grants Commission (UGC), India, for a Research Fellowship. We also thank the Center for Environmental Science and Technology, University of Notre Dame, for the mass analysis, supported by the NSF under Grant CHE-0741793.

■ REFERENCES

(1) (a) Lipscomb, W. N. *Boron Hydrides*; W. A. Benjamin: New York, 1963. (b) Olah, G. A.; Wade, K.; Williams, R. E. *Electron Deficient Boron and Carbon Clusters*; John Wiley and Sons: New York, 1991.

(2) (a) Schleyer, P. v. R.; Subramanian, G.; Jiao, H.; Najafian, K.; Hofmann, M. In *Advances in Boron Chemistry*; Siebert, W., Ed.; The Royal Society of Chemistry: Cambridge, U.K., 1997. (b) Schleyer, P. v. R.; Najafian, K. In *The Borane, Carborane, Carbocation Continuum*; Casanova, J., Ed.; Wiley: New York, 1998.

(3) (a) Brown, L. D.; Lipscomb, W. N. *Inorg. Chem.* **1977**, *16*, 2989−2996. (b) Lipscomb, W. N.; Massa, L. *Inorg. Chem.* **1992**, *31*, 2297−2299.

(4) (a) Schleyer, P. v. R.; Najafian, K.; Mebel, A. M. *Inorg. Chem.* **1998**, *37*, 6765−6772. (b) Wang, Z. X.; Schleyer, P. v. R. *J. Am. Chem. Soc.* **2003**, *125*, 10484−10485.

(5) (a) Saxena, A. K.; Hosmane, N. S. *Chem. Rev.* **1993**, *93*, 1081−1124. (b) Grimes, R. N. *Coord. Chem. Rev.* **2000**, *200*−*202*, 773−811.

(6) (a) Zhang, J.; Xie, Z. *Chem.—Asian J.* **2010**, *5*, 1742−1757. (b) Deng, L.; Xie, Z. *Coord. Chem. Rev.* **2007**, *251*, 2452−2476. (c) Deng, L.; Zhang, J.; Chan, H.-S.; Xie, Z. *Angew. Chem., Int. Ed.* **2006**, *45*, 4309−4313.

(7) (a) Burke, A.; Ellis, D.; Giles, B. T.; Hodson, B. E.; Macgregor, S. A.; Rosair, G. M.; Welch, A. J. *Angew. Chem., Int. Ed.* **2003**, *42*, 225−228. (b) McIntosh, R. D.; Ellis, D.; Rosair, G. M.; Welch, A. J. *Angew. Chem., Int. Ed.* **2006**, *45*, 4313−4316.

(8) Jemmis, E. D.; Kumar, P. N. V. P.; Sastry, G. N. *Polyhedron* **1990**, *9*, 2359−2370.

(9) Kudinov, A. R.; Perekalin, D. S.; Rynin, S. S.; Lyssenko, K. A.; Grintselev-Knyazev, G. V.; Petrovskii, P. V. *Angew. Chem., Int. Ed.* **2002**, *41*, 4112−4114.

(10) Roy, D. K.; Bose, S. K.; Anju, R. S.; Mondal, B.; Ramkumar, V.; Ghosh, S. *Angew. Chem., Int. Ed.* **2013**, *52*, 3222−3226.

(11) (a) Fehlner, T. P.; Halet, J.-F.; Saillard, J.-Y. *Molecular Clusters. A Bridge to Solid-State Chemistry*; University Press: Cambridge, U.K., 2007. (b) Housecroft, C. E. In *Inorganometallic Chemistry*; Fehlner, T. P., Ed.; Plenum: New York, 1992. (c) Ghosh, S.; Lei, X.; Shang, M.; Fehlner, T. P. *Inorg. Chem.* **2000**, *39*, 5373−5382. (d) Ghosh, S.; Shang, M.; Fehlner, T. P. *J. Organomet. Chem.* **2000**, *614*−*615*, 92−98.

(12) (a) Kennedy, J. D. *Prog. Inorg. Chem.* **1984**, *32*, 519−670. (b) Kennedy, J. D. *Prog. Inorg. Chem.* **1986**, *34*, 211−434.

(13) Greenwood, N. N.; Ward, I. M. *Chem. Soc. Rev.* **1974**, *3*, 231−271.

(14) Barton, L.; Srivastava, D. K. In *Comprehensive Organometallic Chemistry II*; Abel, E. W., Stone, F. G. A., Wilkinson, G., EDs.; Pergamon: Oxford, U.K., 1995; Vol. *1*.

(15) (a) Mingos, D. M. P. *Nature (London) Phys. Sci.* **1972**, *236*, 99−102. (b) Wade, K. *Inorg. Nucl. Chem. Lett.* **1972**, *8*, 559−563. (c) Wade, K. *Adv. Inorg. Chem. Radiochem.* **1976**, *18*, 1−66.

(16) (a) Le Guennic, B.; Jiao, H.; Kahlal, S.; Saillard, J.-Y.; Halet, J.-F.; Ghosh, S.; Shang, M.; Beatty, A. M.; Rheingold, A. L.; Fehlner, T. P. *J. Am. Chem. Soc.* **2004**, *126*, 3203−3217. (b) Ghosh, S.; Noll, B. C.; Fehlner, T. P. *Angew. Chem., Int. Ed.* **2005**, *44*, 2916−2918. (c) Bould, J.; Kennedy, J. D. *Chem. Commun.* **2004**, 2380−2381. (d) Bould, J.; Kennedy, J. D. *Chem. Commun.* **2008**, 2447−2449.

(17) (a) Dunks, G. B.; McKown, M. M.; Hawthorne, M. F. *J. Am. Chem. Soc.* **1971**, *93*, 2541−2543. (b) Maxwell, W. M.; Weiss, R.; Sinn, E.; Grimes, R. N. *J. Am. Chem. Soc.* **1977**, *99*, 4016−4029.

(18) (a) Ghosh, S.; Fehlner, T. P.; Beatty, A. M. *Chem. Commun.* **2005**, 3080−3082. (b) Bose, S. K.; Ghosh, S.; Noll, B. C.; Halet, J.-F.; Saillard, J.-Y.; Vega, A. *Organometallics* **2007**, *26*, 5377−5385.

(19) Lei, X.; Shang, M.; Fehlner, T. P. *Angew. Chem., Int. Ed.* **1999**, *38*, 1986−1989.

(20) (a) Roy, D. K.; Bose, S. K.; Anju, R. S.; Ramkumar, V.; Ghosh, S. *Inorg. Chem.* **2012**, *51*, 10715−10722. (b) Lei, X.; Shang, M.; Fehlner, T. P. *J. Am. Chem. Soc.* **1999**, *121*, 1275−1287. (c) Yan, H.; Beatty, A. M.; Fehlner, T. P. *Organometallics* **2002**, *21*, 5029−5037.

(21) (a) Roy, D. K.; Bose, S. K.; Geetharani, K.; Chakrahari, K. K. V.; Mobin, S. M.; Ghosh, S. *Chem.—Eur. J.* **2012**, *18*, 9983−9991. (b) Bose, S. K.; Geetharani, K.; Ramkumar, V.; Varghese, B.; Ghosh, S. *Inorg. Chem.* **2010**, *49*, 2881−2888. (c) Dhayal, R. S.; Chakrahari, K. K. V.; Varghese, B.; Mobin, S. M.; Ghosh, S. *Inorg. Chem.* **2010**, *49*, 7741−7747.

(22) (a) Bose, S. K.; Geetharani, K.; Varghese, B.; Mobin, S. M.; Ghosh, S. *Chem.—Eur. J.* **2008**, *14*, 9058−9064. (b) Bose, S. K.; Geetharani, K.; Ramkumar, V.; Mobin, S. M.; Ghosh, S. *Chem.—Eur. J.* **2009**, *15*, 13483−13490. (c) Geetharani, K.; Bose, S. K.; Varghese, B.; Ghosh, S. *Chem.—Eur. J.* **2010**, *16*, 11357−11366. (d) Geetharani, K.; Bose, S. K.; Sahoo, S.; Ghosh, S. *Angew. Chem., Int. Ed.* **2011**, *50*, 3908−3911.

(23) (a) Wilson, N. M. M.; Ellis, D.; Buoyd, A. S. F.; Giles, B. T.; Macgregor, S. A.; Rosair, G. M.; Welch, A. J. *Chem. Commun.* **2002**, 464−465. (b) Wang, S.; Li, H.-W.; Xie, Z. *Organometallics* **2004**, *23*, 3780−3787. (c) Khattar, R.; Knobler, C. B.; Hawthorne, M. F. *J. Am. Chem. Soc.* **1990**, *112*, 4962−4963. (d) Ellis, D.; Lopez, M. E.; McIntosh, R.; Rosair, G. M.; Welch, A. J. *Chem. Commun.* **2005**, 1917−1919.

(24) Sevov, S. C.; Corbett, J. D. *Inorg. Chem.* **1992**, *31*, 1895−1901.

(25) Mattes, R.; Tebbe, K. F.; Neidhard, H.; Rethfeld, H. *J. Less-Common Met.* **1976**, *47*, 29−32.

(26) Vlasse, M.; Slack, G. A.; Garbauskas, M.; Kasper, J. S.; Viala, J. C. *J. Solid State Chem.* **1986**, *63*, 31−45.

(27) (a) Muetterties, E. L.; Wright, C. M. *Quart. Rev. Chem. Soc.* **1967**, *21*, 109−194 , and references therein, especially pp 175−177. (b) Bergman, G.; Waugh, J. L. T.; Pauling, L. *Acta Crystallogr.* **1957**, *10*, 254−259.

(28) (a) Bould, J.; Greenwood, N. N.; Kennedy, J. D.; McDonald, W. S. *J. Chem. Soc., Chem. Commun.* **1982**, 465−467. (b) Shameema, O.; Jemmis, E. D. *Inorg. Chem.* **2009**, *48*, 7818−7827.
(29) King, R. B. *J. Am. Chem. Soc.* **1969**, *91*, 7211.
(30) Note that **2a**, a derivative of $[B_{15}H_{15}]$ in which the six connected boron atoms are replaced by CpRh, displays the highest stability (Supporting Information, Figures S1, S4 and S5).
(31) Ghosh, S.; Shang, M.; Li, Y.; Fehlner, T. P. *Angew. Chem., Int. Ed.* **2001**, *40*, 1125−1128.
(32) Sheldrick, G. M. *SHELXS-97*; University of Göttingen: Göttingen, Germany, 1997.
(33) Ditzel, E. J.; Fontaine, X. L. R.; Fowkes, H.; Greenwood, N. N.; Kennedy, J. D.; MacKinnon, P.; Sisan, Z.; Thornton-Pett, M. *J. Chem. Soc., Chem. Commun.* **1990**, 1692−1694.
(34) Fontaine, X. L. R.; Fowkes, H.; Greenwood, N. N.; Kennedy, J. D.; Thornton-Pett, M. *J. Chem. Soc., Chem. Commun.* **1985**, 1722−1723.
(35) (a) Sahoo, S.; Dhayal, R. S.; Varghese, B.; Ghosh, S. *Organometallics* **2009**, *28*, 1586−1589. (b) Sahoo, S.; Mobin, S. M.; Ghosh, S. *J. Organomet. Chem.* **2010**, *695*, 945−949.
(36) (a) Gallahan, K. P.; Evans, W. J.; Lo, F. Y.; Strouse, C. E.; Hawthorne, M. F. *J. Am. Chem. Soc.* **1975**, *97*, 296. (b) Jung, C. W.; Baker, R. T.; Knobler, C. B.; Hawthorne, M. F. *J. Am. Chem. Soc.* **1980**, *102*, 5782−5790. (c) Jung, C. W.; Baker, R. T.; Hawthorne, M. F. *J. Am. Chem. Soc.* **1981**, *103*, 810−816.
(37) (a) Bould, J.; Greenwood, N. N.; Kennedy, J. D.; McDonald, W. S. *J. Chem. Soc., Chem. Commun.* **1982**, 465−467. (b) Crook, J. E.; Elrington, M.; Greenwood, N. N.; Kennedy, J. D.; Thornton-Pett, M.; Woollins, J. D. *J. Chem. Soc., Dalton Trans.* **1985**, 2407−2415.
(38) Ryschkewitsch, G. E.; Nainan, K. C. *Inorg. Synth.* **1974**, *15*, 113−114.
(39) Altornare, A.; Cascarano, G.; Giacovazzo, C.; Guagliardi, A. *J. Appl. Crystallogr.* **1993**, *26*, 343−350.
(40) Sheldrick, G. M. *SHELXL-97*; University of Göttingen: Göttingen, Germany, 1997.
(41) Koch, W.; Holthausen, M. C. *A Chemist's Guide to Density Functional Theory*; Wiley-VCH: Weinheim, Germany, 2000.
(42) Frisch, M. J.; Trucks, G. W.; Schlegel, H. B.; Scuseria, G. E.; Robb, M. A.; Cheeseman, J. R.; Scalmani, G.; Barone, V.; Mennucci, B.; Petersson, G. A. ; Nakatsuji, H.; Caricato, M.; Li, X., Hratchian, H. P.; Izmaylov, A. F.; Bloino, J.; Zheng, G.; Sonnenberg, J. L.; Hada, M.; Ehara, M.; Toyota, K.; Fukuda, R.; Hasegawa, J.; Ishida, M.; Nakajima, T.; Honda, Y.; Kitao, O.; Nakai, H.; Vreven, T.; Montgomery, J. A.; Jr., Peralta, J. E.; Ogliaro, F.; Bearpark, M.; Heyd, J. J.; Brothers, E.; Kudin, K. N.; Staroverov, V. N.; Keith, T.; Kobayashi, R.; Normand, J.; Raghavachari, K.; Rendell, A.; Burant, J. C.; Iyengar, S. S.; Tomasi, J.; Cossi, M.; Rega, N.; Millam, J. M.; Klene, M.; Knox, J. E.; Cross, J. B.; Bakken, V.; Adamo, C.; Jaramillo, J.; Gomperts, R.; Stratmann, R. E.; Yazyev, O.; Austin, A. J.; Cammi, R.; Pomelli, C.; Ochterski, J. W.; Martin, R. L.; Morokuma, K.; Zakrzewski, V. G.; Voth, G. A.; Salvador, P.; Dannenberg, J. J.; Dapprich, S.; Daniels, A. D.; Farkas, O.; Foresman, J. B.; Ortiz, J. V.; Cioslowski, J.; Fox, D. J. *Gaussian 09*, Revision C.01; Gaussian, Inc.: Wallingford, CT, 2010.
(43) (a) Schmider, H. L.; Becke, A. D. *J. Chem. Phys.* **1998**, *108*, 9624−9631. (b) Perdew, J. P. *Phys. Rev. B* **1986**, *33*, 8822−8824.
(44) Weigend, F.; Ahlrichs, R. *Phys. Chem. Chem. Phys.* **2005**, *7*, 3297−3305.
(45) Andrae, D.; Häußermann, U.; Dolg, M.; Stoll, H.; Preuss, H. *Theor. Chim. Acta* **1990**, *77*, 123−141.
(46) Schleyer, P. v. R.; Maerker, C.; Dransfeld, A.; Jiao, H.; Hommes, N. J. R. v. E. *J. Am. Chem. Soc.* **1996**, *118*, 6317−6318.
(47) Chen, Z.; Wannere, C. S.; Cominboeuf, C.; Puchta, R.; Schleyer, P. v. R. *Chem. Rev.* **2005**, *105*, 3842−3888.
(48) (a) Becke, A. D. *Phys. Rev. A* **1988**, *38*, 3098−3100. (b) Lee, C.; Yang, W.; Parr, R. G. *Phys. Rev. B* **1988**, *37*, 785−789. (c) Becke, A. D. *J. Chem. Phys.* **1993**, *98*, 5648−5652.
(49) London, F. J. *J. Phys. Radium* **1937**, *27*, 397−409.
(50) Ditchfield, R. *Mol. Phys.* **1974**, *27*, 789−807.
(51) Wolinski, K.; Hinton, J. F.; Pulay, P. *J. Am. Chem. Soc.* **1990**, *112*, 8251−8260.
(52) Schreckenbach, G.; Ziegler, T. *J. Phys. Chem.* **1995**, *99*, 606−611.
(53) Schreckenbach, G.; Ziegler, T. *Int. J. Quantum Chem.* **1997**, *61*, 899−918.
(54) Schreckenbach, G.; Ziegler, T. *Int. J. Quantum Chem.* **1996**, *60*, 753−766.
(55) Wolff, S. K.; Ziegler, T. *J. Chem. Phys.* **1998**, *109*, 895−905.
(56) Wolff, S. K.; Ziegler, T.; van Lenthe, E.; Baerends, E. J. *J. Chem. Phys.* **1999**, *110*, 7689−7698.
(57) Bader, R. F. W. *Atoms in Molecules: A Quantum Theory*, 2nd ed.; Clarendon: Oxford, U.K., 1990.